Beam-beam-as-wire and wire-as-octupole approximations: tuneshifts
TRI-DN-BB-20-25

Dobrin Kaltchev

ARTICLE HISTORY
Compiled August 23, 2022

1. Introduction

Tuneshifts (detunings) and structure of the footprint wing are discussed. We consider three cases:

(1) A Long-range beam-beam (bb) collision. The bb optical element is installed in some sample lattice (weak+strong-beams) so that it resembles an arbitrary collision occurring in IR5, Left. The full separation is $D_x < 0$ in the horizontal plane.
(2) An ideal wire-corrector element (aka wire) derived from the bb element (1) by taking vanishing strong-beam r.m.s. sizes $\sigma_{x,y}^{\mathrm{str}}$ of the strong beam.
(3) A thin octupole installed in the weak beam at the lattice location corresponding to either (1) or (2).

One goal is to compare the analytic formulae [3] describing the tuneshift with MadX tracking. The nearly-horizontal ("H") wing of the footprint is mostly of interest and its structure at high amplitudes a_x, up to the strong-beam axis (same as the amplitude at which the wire is set). The full range of amplitudes is then $a < a_x < a_x^{\mathrm{max}} = D_x/\sigma_x^{\mathrm{wk}}$.

Another is to compare the "mapping transforms" generating the H wing. That is, if the point transformation from initial-amplitude space to tune space were to be the same for all cases 1-3, then this would greatly simplify the correction of the bb with wire and the replacement of the wire with octupole.

For this, assume that the initial-amplitude space is in the vicinity of the separation plane uniformly populated in radial direction. Then, as we will see, the above similarity is not fulfilled – the three transforms are in general different and coincide only at small amplitudes:

The transform for bb differs with the one for a wire only at high amplitudes – 2-3 sigma from the core.

For (3), the b_3 of the octupole can be so chosen that the latter becomes equivalent to a hypothetical wire, for which only the 4th order terms in the potential are retained. Thus, in such case, (2) and (3) produce the same detunings. On the other hand, for a realistic wire, one must also include the higher terms in the wire potential (16th order turns out to be needed, in order for it to agree with tracking over almost the entire a_x range). Therefore, the H wing generated by a realistic wire is much more extended in tune space that the one of the equivalent octupole. Thus, the wire and octupole transforms are identical only at relatively low amplitudes ~ 3.5 and differ strongly at higher amplitudes.

The three ranges of agreement can be approximately determined from the presented plots.

2. Lattice and initials for tracking

The tracking procedure is the same as in [1]: a sample-ring lattice (weak beam) is created containing a straight section with a horizontal closed-orbit (CO) bump inside this section. Within

the bump, we install a thin octupole (K3L, b3 = KRL/6) and, at the same location, a beam-beam element (full separation D_x, strong-beam sigmas $\sigma^{\mathtt{str.}}_{x,y}$, bunch population N_b). The weak-beam is ultra-relativistic with $\gamma \gg 1$. The CO bump is controlled with a parameter xing and collapses to zero when xing$= 0$.

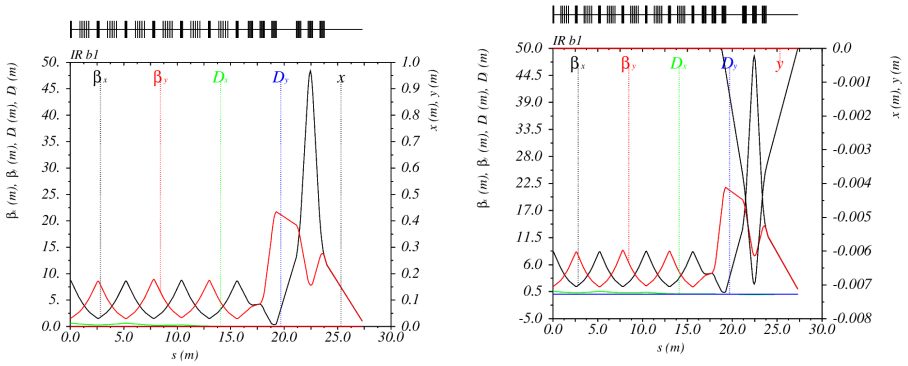

Figure 1. The test-ring lattice section designed to resemble IR5 Left; without CO bump (left) and with a negative bump (right). The bb location is $s = -4$ m from the IP, i.e. from the section end.

A simplified uniform initial distribution in amplitude space is used: the initial points are chosen equidistant along two lines in x, y space and hence along similar lines in $a_{x,y}$, Figure 2, left.

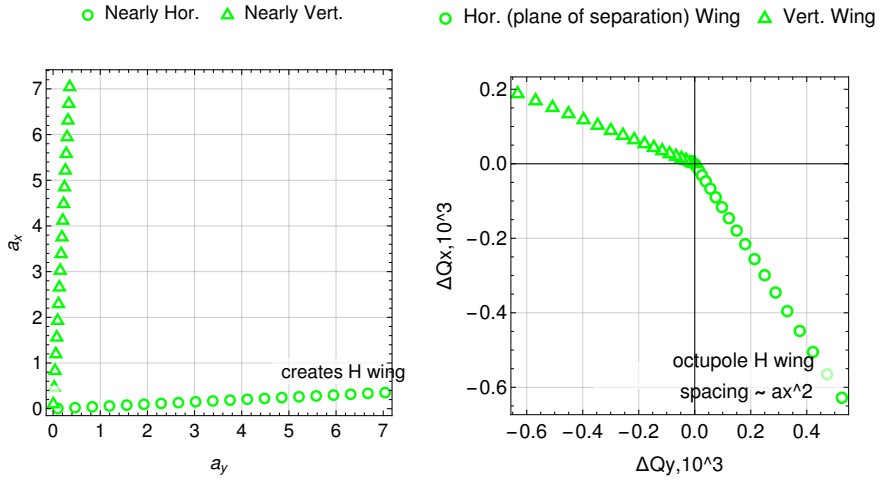

Figure 2. Left: initials for tracking – the nearly horizontal line is the source for the H wing. Right: octupole footprint.

3. Octupole (3)

A thin octupole is in Mad defined as bb_oct:multipole,knl:={0,0,0,K3L}. It correspond to the kick Hamiltonian (Lie-exponent factor): $1/4!K3L\ Re[(x+iy)^4$ with the coefficient multiplying x^4 being $1/24K3L$ and hence $b_3 = K3L/6$.

We turn the bump off and track the initials Fig 2, left, for 2000 turns. Only the octupole is present. There is a nearly exact agreement between MadX tracking (dynaptune) and the formula for octupole detunings

$$\frac{3b_3}{4}(\beta_x^2 J_x - 2\beta_x J_x J_y) \quad \text{and} \quad x \leftrightarrow y \tag{3.1}$$

($\beta_{x,y} \equiv \beta^{\mathrm{wk}}_{x,y}$) as this is seen on Fig 3 (H wing only).

Since $J_x = \frac{a_x^2}{2}\varepsilon$ and ΔQ_x is linear in $\sim J_{x,y}$, the wings are less populated at higher amplitudes (spacing between points increasing quadratically with amplitude).

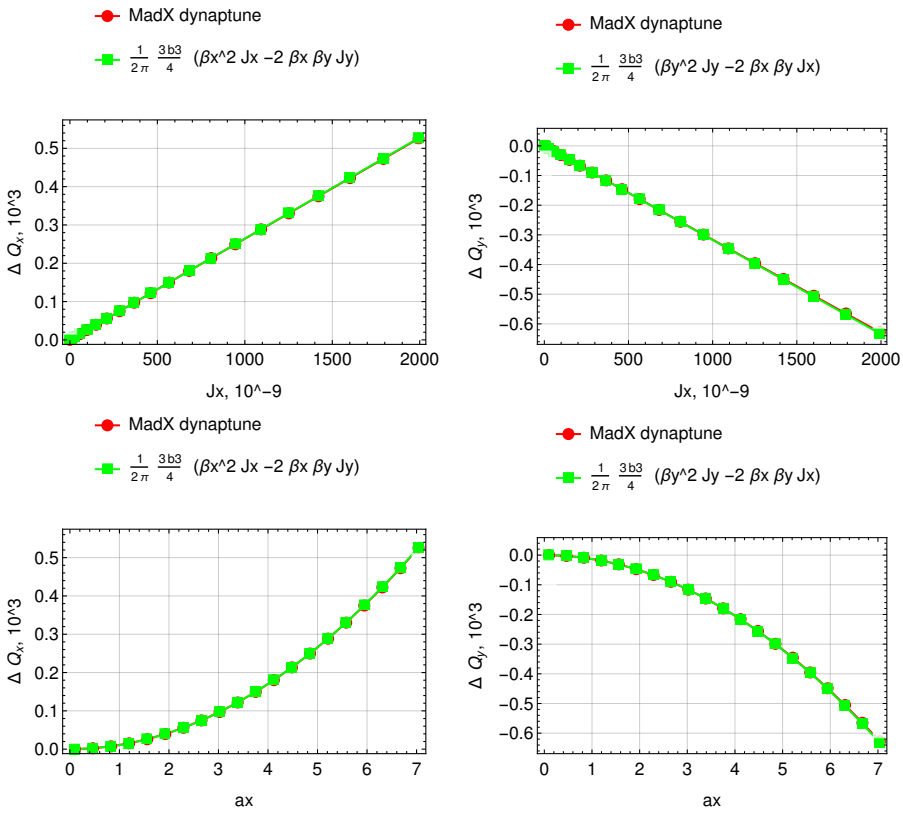

Figure 3. Octupole H wing: agreement between analytic tuneshift formula with tracking on either action j_x or amplitude (a_x) axes.

4. Beam-beam and "wire as beam-beam"

The horizontal/vertical analytic detunings are given by these derivatives of the averaged (over phases) beam-beam Hamiltonian:

$$\begin{aligned} \Delta Q_z(a_x,a_y) &= \frac{2\xi}{a_z}\frac{\partial < H_{\rm bb} >_{\phi_{x,y}}}{\partial a_z}, \\ <>_{\phi_{x,y}} &\equiv \frac{1}{4\pi^2}\iint_0^{2\pi} d\phi_x d\phi_y \end{aligned} \tag{4.2}$$

where $z = x, y$ and $\xi \equiv \frac{N_b r_0}{4\pi\gamma\varepsilon}$ is the beam-beam parameter. Assume that the 2D-Bessel function has been encoded (in, say, *Mathematica* or `Python`):

$$\begin{aligned} \mathbf{I}_n(u_1,u_2) &\equiv \sum_{q=-\infty}^{\infty} I_{n-2q}(u_1) I_q(u_2) = \\ &= \frac{i^{-n}}{2\pi} e^{-u_2}\int_0^{2\pi} e^{-i\,n\,\phi - u_1 \sin\phi + 2\,u_2 \sin^2\phi} d\phi. \end{aligned} \tag{4.3}$$

Here ∞ is replaced by $q_{\rm max} \sim 30-40$. Then ΔQ_z can be computed as an integral over a 2D-Bessel kernel. It may be:

– a t-integral derived and used in [2];

– a path integral in ξ parametrizaton [3] – this is Eq. 4.5 below;

– a regular (not a path-) integral in ξ parametrizaton [3] – these are Eqns. 4.7, 4.8 below.

The plan is to use the ξ-integral forms (last two) as they can describe both the case of a beam-beam (1) and of an ideal wire (2). Besides amplitudes $a_{x,y}$, these forms depend on the initial slopes of the integration path, see [3], and the flatness parameter r:

$$\psi_x \equiv \frac{d_x}{r a_x}; \quad \psi_y \equiv \frac{a_y}{r a_x}; \quad r \equiv \frac{\sigma_y^{\rm str}}{\sigma_x^{\rm str}}. \tag{4.4}$$

Here $d_x = \frac{D_x}{\sigma_x^{\rm str}}$. Thus, only the strong-beam lattice parameters are relevant. For an exactly asymmetric weak and strong beams at this location, one has:

$$\sigma_{x,y}^{\rm wk} = \sigma_{y,x}^{\rm str}$$

Then ψ_x and r can be expressed in terms of weak-beam parameters:

$$\psi_x = \frac{D_x}{\sigma_x^{\rm wk} a_x}, \quad r = \frac{\sigma_x^{\rm wk}}{\sigma_y^{\rm wk}},$$

where ψ_x now has the meaning of (inverted) distance of the particle to the strong-beam core.

The path-integral form is:

$$\begin{aligned}
&\Delta Q_z(a_x, a_y; d_x, r) = -\frac{2}{a_x^2}\int_0^{r a_x} \xi\,\eta_z\,\mathbf{T}^z\,d\xi \\
&\mathbf{T}^x = e^{U_2^x+U_3^x+U_2^y+U_3^y}\mathbf{I}_0(U_1^y, U_2^y)\left(\mathbf{I}_0(U_1^x, U_2^x) + \mathbf{I}_2(U_1^x, U_2^x) + \frac{U_1^x}{2U_2^x}\mathbf{I}_1(U_1^x, U_2^x)\right) \\
&\mathbf{T}^y = \mathbf{T}^x \ \text{ with } x \leftrightarrow y,
\end{aligned} \tag{4.5}$$

where

$$\begin{aligned}
&U_1^x = \psi_x \xi^2, \ U_2^x = -\frac{1}{4}\xi^2, \ U_3^x = -\frac{\psi_x^2 \xi^2}{2}, \\
&U_2^y = -\frac{\psi_y^2 \xi^2}{4 g_r^2}, \ U_2^y = 0, \ U_3^y = 0; \\
&\eta_x \equiv \frac{1}{g_r}, \ \eta_y \equiv \frac{1}{r^2 g_r^3}; \\
&g_r = g_r(\xi, a_x) = \sqrt{(r^2-1)\,\xi^2/(r a_x)^2 + 1}.
\end{aligned} \tag{4.6}$$

This can be rewritten as regular integrals:

$$\begin{aligned}
&\Delta Q_x(a_x, a_y; d_x, r) = \\
&= -\frac{2}{a_x^2}\int_0^{r a_x} \frac{\xi}{g_r}\exp\left[-\frac{\xi^2}{4}\left(1 + 2\psi_x^2 + \frac{\psi_y^2}{g_r^2}\right)\right] \times \left[\mathbf{I}_0\,\mathbf{I}_0 + \mathbf{I}_2\,\mathbf{I}_0 - 2\psi_x \mathbf{I}_1\,\mathbf{I}_0\right] d\xi
\end{aligned} \tag{4.7}$$

$$\begin{aligned}
&\Delta Q_y(a_x, a_y; d_x, r) = \\
&= -\frac{2}{r^2 a_x^2}\int_0^{r a_x} \frac{\xi}{g_r^3}\exp\left[-\frac{\xi^2}{4}\left(1 + 2\psi_x^2 + \frac{\psi_y^2}{g_r^2}\right)\right] \times \left[\mathbf{I}_0\,\mathbf{I}_0 + \mathbf{I}_0\,\mathbf{I}_2 - 2\psi_x \mathbf{I}_0\,\mathbf{I}_1\right] d\xi,
\end{aligned} \tag{4.8}$$

where:

$$\mathbf{I}_m\,\mathbf{I}_k \equiv \mathbf{I}_m(\psi_x\xi^2, -\frac{1}{4}\xi^2)\;\; \mathbf{I}_k(0, -\frac{\psi_y^2\xi^2}{4g_r^2}) \tag{4.9}$$

$m,k = 0,1,2$, and g_r was defined in Eq. 4.6.

An ideal wire can be described as a long-range bb collision with vanishing rms size of the strong beam ("wire-as-bb"). Let us scale down, i.e. divide, both $\sigma_{x,y}^{\rm str}$ by the same factor $f_w \geq 1$. Then either of the above ξ-integral forms can describe the case of a beam-beam (1), by taking $f_w = 1$, or an ideal wire (2), by taking f_w large, say ~ 100. Thus, the ideal-wire tuneshifts are:

$$\Delta Q_z^{\rm w} = f_w^2\,\Delta Q_z(f_w a_x, f_w a_y; f_w d_x, r), \quad f_w = \text{large}, \tag{4.10}$$

and the bb case follows from here for $f_w = 1$. The real-space full separation D_x now plays the role of a physical distance of the wire to the weak-beam axis.

Notice that after the sigma-scaling:

- according to Eq. 4.4, the slopes $\psi_{x,y}$ remain the same;
- according to Eq. 4.6, g_r can be, with an excellent accuracy, replaced with unity.
- the upper bound on integration ra_x can be replaced with infinity – a "full escape" from the strong-beam core, [3].

The result from the tracking test is shown on Figure 4. Here $g_r = 1$. The same initials are used as for the octupole, i.e. Fig 1, left. The only disagreement is at the last point of the H-wing generated by wire, i.e amplitude $a_x = a_x^{\rm max}$. Tracking has failed at this point.

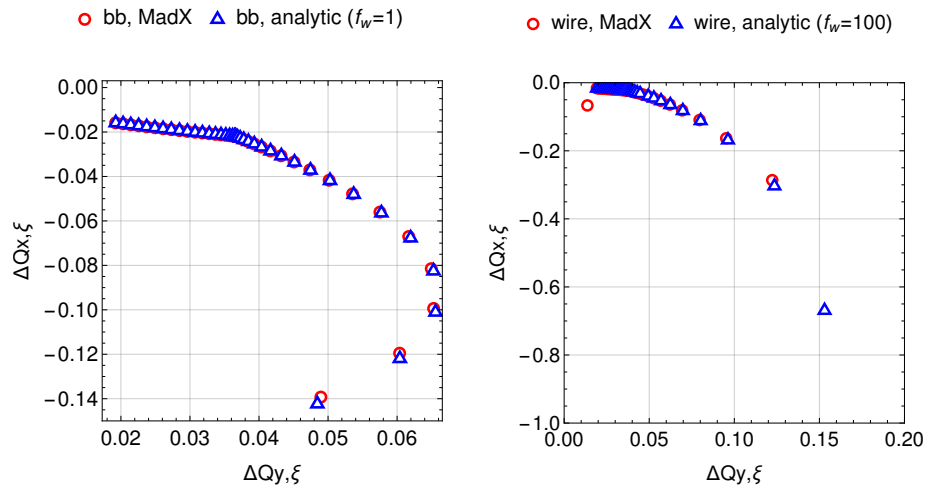

Figure 4. Agreement between MadX and the analytic detunings Eq. 4.10 for beam-beam, $f_w = 1$ (left plot) and ideal wire, $f_w = 100$ (right plot). The $a_{x,y}$ are as on Fig 1, left. Here there is no correction for zero-amplitude tune and tune-shifts are normalized to the bb parameter, in this case $\xi = 0.2$.

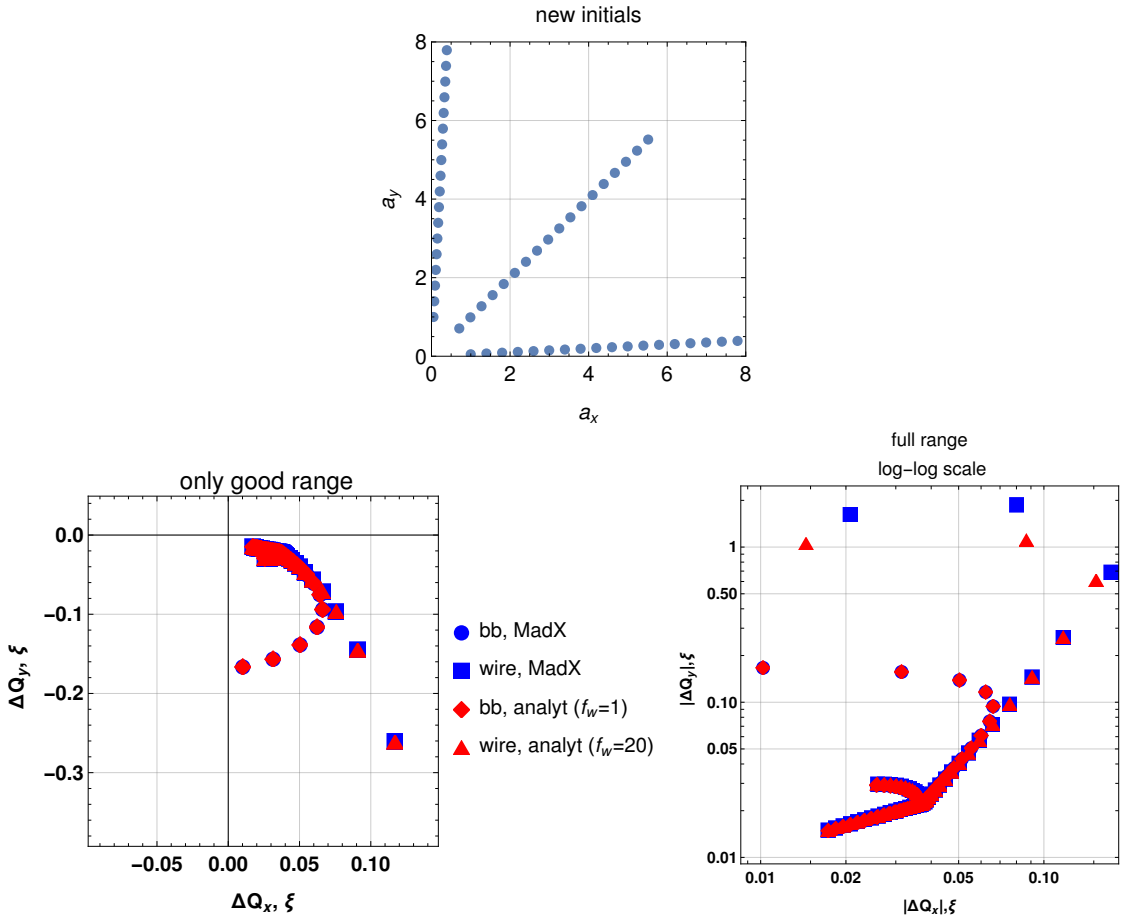

Figure 5. Same as Fig 4, i.e. agreement between MadX and the analytic detunings Eq. 4.10. Here for a new set of initial amplitudes (top)

On Figure 5, the maximum amplitude is extended up to 8σ, i.e. past the strong beam core while preserving the step in amplitude. As it happens, there is no initial starting amplitude that is exactly on the strong-beam core. Therefore no large discrepancies are seen between tracking and formula Eq. 4.10. Also the set of initial amplitudes has been appended with ones near diagonal $a_x = a_y$, and a smaller f_w is used describing the wire: $f_w = 20$ instead of 100.

5. Wire detuning derived from expanded potential

There is an alternative way of computing the wire detuning that produces the same result as Eq. 4.10 above. Recall that, to derive Eq. 4.10, we substituted vanishing r.m.s. beam sizes in the beam-beam tuneshifts. This could have been done from the start, i.e. in the original beam-beam Hamiltonian. This result [3] is an expression for the ideal-wire potential $-H_{\mathrm{w}}$ (also one of a thin pencil strong beam). This ideal-wire potential, [3], is simply a logarithm:

$$-H_{\mathrm{w}} = -\ln\left((D_x + x)^2 + y^2\right). \tag{5.11}$$

According to Eq. 4.2, one can derive the wire detuning by averaging this expression over phases:

$$\Delta Q_z^{\mathrm{w}}(a_x, a_y) = \frac{2\xi}{a_z} \frac{\partial < H_{\mathrm{w}} >_{\phi_{x,y}}}{\partial a_z}, . \tag{5.12}$$

The logarithm, with subtracted its quadratic terms in x, y, is first expanded in power series to order $N_{\texttt{taylor}}$, where x, y are the ones describing the unperturbed trajectory:

$$\ln\left((D_x+x)^2+y^2\right)-\frac{-x^2+y^2}{D_x^2}=\sum_{m,k}^{N_{\texttt{taylor}}} a_{mk}x^m y^k \tag{5.13}$$
$$x=\sqrt{2\beta_x^{\texttt{wk}}J_x}\sin\phi_x \quad y=\sqrt{2\beta_y^{\texttt{wk}}J_y}\sin\phi_y$$

and averaging over phases is performed with *Mathematica*.

The tracking test (MadX `dynaptune`), Figure 6, is performed only for the near-horizontal H wing. For the Taylor-expansion tune-shift to agree with tracking for as large a_x as possible, one needs to take $N_{\texttt{taylor}} \geq 16 . a_x \sim a_x^{\max}$. A Taylor expansion of any order however would diverge for a_x taken exactly on the strong-beam core. Finally, in this comparison, the linear terms in the potential have been subtracted, see above. Hence the tune-shifts vanish at the origin $a_{x,y}=0$ and hence, before tracking, the ring tunes need be matched to the unperturbed ones, in absence of wire.

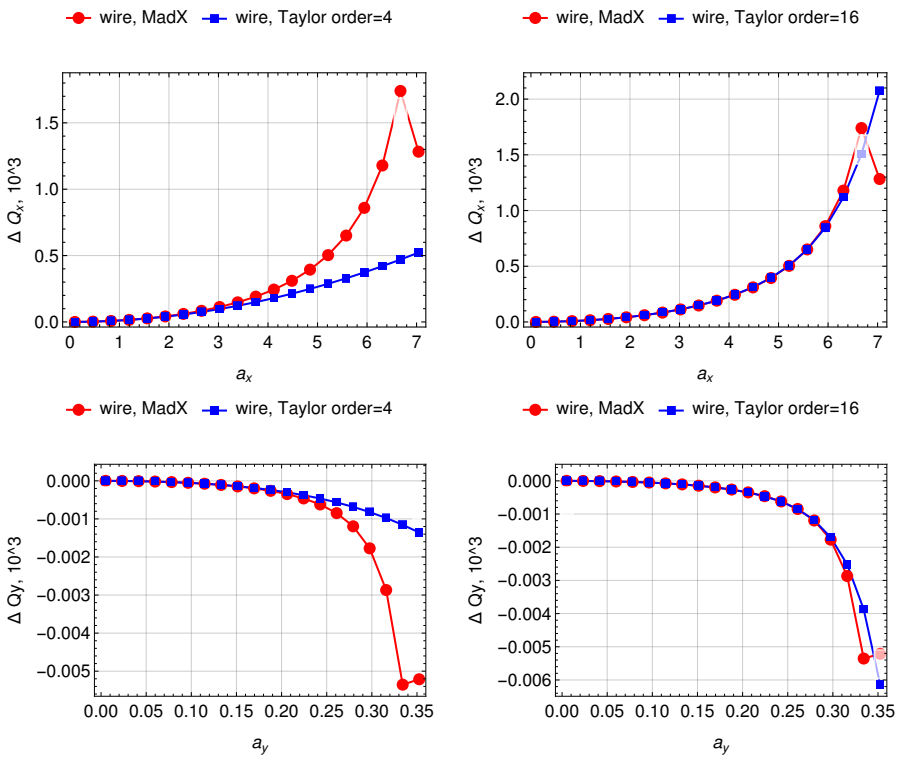

Figure 6. Wire H wing: verification of the detuning-via-Taylor method Eq. 5.12 with tracking. The wire detuning (same as the H wing on Figure 4, right) is compared with the result from Eq. 5.12 for two maximum orders $N_{\texttt{taylor}}=4$ and $N_{\texttt{taylor}}=16$. can account for the last point, see the text.

6. Wire as octupole

Let $b_3^{\texttt{EQUIV}}$ be the equivalent octupole b_3 produced by the ideal wire, i.e. for a wire-potential expansion with $N_{\texttt{taylor}}=4$. The tune-shifts are:

$$\frac{3b_3^{\texttt{EQUIV}}}{8\pi}(\beta_x^2 J_x - 2\beta_x J_x J_y) \quad \text{and} \quad x \leftrightarrow y \tag{6.14}$$

$$b_3^{\texttt{EQUIV}} = \frac{N_b r_0}{\gamma}\frac{2}{D_x^4} \tag{6.15}$$

Figure 7 compares ΔQ_x for the H wing for three cases: equivalent-octupole tracking, the analytic formula, and the realistic wire (order 16). Evidently, the higher order terms $N_{\texttt{taylor}} > 4$ in the wire-potential expansion cause additional tune-shift at high amplitudes. Clearly, the wire and octupole tune-mapping transforms are identical up to amplitudes ~ 3.5 (in σ_x^{wk}) and differ strongly at higher amplitudes.

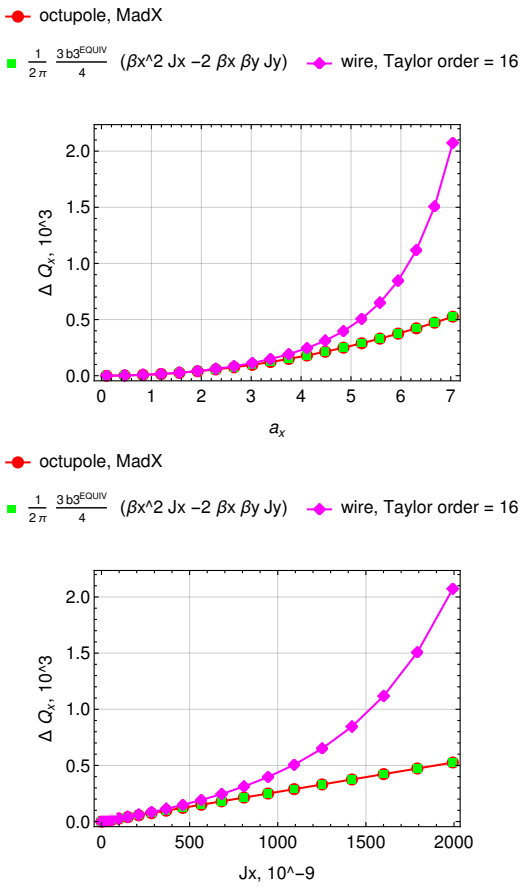

Figure 7. Comparison between the "wire-as-octupole" model and realistic wire in terms of horizontal amplitude (top), or action (bottom).

7. All three cases – footprint

We are now in a position to compare the three footprints a bb element, an ideal-wire, and a thin octupole, whose strength is equivalent to the octupole terms in the expansion of the wire-potential. The result is shown on Figure 8.

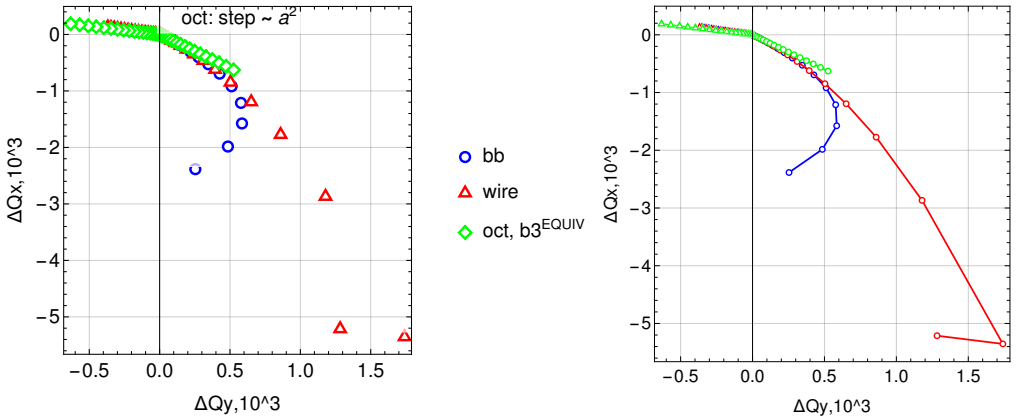

Figure 8. Footprints for back-to-back installed: bb, wire and equivalent octupole. The initial amplitudes are as on Figure 2, left.

8. Summary

Analytic formulas for the tuneshift of a long-range bb and ideal wire were presented.

In a test lattice, the ideal wire was installed back-to-back with the long-range bb effectively replacing the strong beam at this location, i.e. same full separation and effective charge. Also a case when the wire is replaced with a thin octupole with strength equivalent to the wire octupole component was considered.

The analytic formulas were found to agree with MadX tracking for all three cases.

Also the footrint wing created the collision plane was compared Fig 8 for all three cases.

We found that, with full separation 7.3 sigma, the wire would be able to compensate the tune-shift generated by the bb up to $5.5-6$ sigma since the wing structure is nearly the same.

It was found that the ability of the octupole to mimic this compensating action of the wire is more limited. This was explained with the absence of higher order terms > 4 in the octupole potential.

References

[1] Dobrin Kaltchev, General Beam-beam detuning formula and its tests, TRI-BN-22-20
[2] D. Kaltchev, *Fourier Coefficients of Long-Range Beam-Beam Hamiltonian via Two-Dimensional Bessel functions* Proc. of IPAC 2018, Vancouver BC, Canada
[3] D. Kaltchev, *Beam-beam resonance driving terms via Two-dimensional Bessel functions. Application to wire correction in the HL-LHC.* in preparation